Journal of Membrane Science 428 (2013) 470–479

Contents lists available at SciVerse ScienceDirect

Journal of Membrane Science

journal homepage: www.elsevier.com/locate/memsci

Stable and hydroxide ion conductive membranes for fuel cell applications: Chloromethyaltion and amination of poly(ether ether ketone)

Amaranadh Jasti, S. Prakash, Vinod K. Shahi *

Electro-Membrane Processes Division, Central Salt and Marine Chemicals Research Institute, Council of Scientific & Industrial Research (CSIR), G.B. Marg, Bhavnagar-364002, Gujarat, India

ARTICLE INFO

Article history:
Received 29 September 2012
Received in revised form
5 November 2012
Accepted 8 November 2012
Available online 19 November 2012

Keywords:
Poly(ether ether ketone)
Alkaline membrane
Partial sulfonation
Desulfonation
H_2/air alkaline fuel cell

ABSTRACT

Poly(ether ether ketone) (PEEK) was dissolved in conc. H_2SO_4 and its chloromethylation was achieved in presence of paraformaldehyde, trimethylchlorosilane and Lewis acid catalyst, obtained about 35–75% degree of chloromethylation (DCM). This idea is based on partial sulfonation of PEEK to make it soluble and further complete replacement of $-SO_3H$ with $-CH_2Cl$ groups. Alkaline membranes (AMs) were prepared by quaternization of chloromethylated PEEK (CMPEEK). The reported method is a "green" alternative for the production of AEM without the use of hazardous chemicals (such as chloromethyl methyl ether, chloromethyloctylether, *bis*(chloromethyl) ether etc.). Chronopotentiometry study of prepared membranes confirmed their homogeneous and alkaline nature suitable for methanol fuel cells. The AMs exhibit a splendid chemical stability at 10 M KOH. Alkaline conductivity of quaternized poly(ether ether ketone) membrane with 75% DCM (QPEEK-75) (14.63 mS cm^{-1}) in equilibration with deionized water was relatively high in compare with other AMs reported in the literature. For the H_2/air single fuel cell at 50 °C with QPEEK-75 membrane, about 1.02 V OCV and 48.09 mW cm^{-2} power density at 109.3 mA cm^{-2} current density were obtained.

1. Introduction

Proton exchange membrane fuel cells (PEMFCs) are promising energy conversion devices due to their high energy-conversion efficiency, power density, and low pollutant emission [1–3]. However, high cost, fuel loss and low durability of the electro catalysts in PEMFCs hampered their commercialisation [4,5]. Recently, significant attention has been rendered for alkaline membrane fuel cells (AMFCs), because of their potential to solve fundamental problems of PEMFCs [6–9]. In AMFCs, alkaline membranes (AMs) serve as hydroxide (OH^-) conductor and separator for fuel and oxidant. Several types of polymers, such as poly(2,6-dimethyl-1,4-phenylene oxide) (PPO), copolymer of chloromethylstyrene and divinylbenzene, PVDF-vinylbenzyl chloride, and poly(vinyl alcohol)–poly(1,3-diethyl-1–1-vinyl imidazolium bromide), grafted poly(hexafluoropropylene-*co*-tetrafluoroethylene) (FEP) [10,11], and copolymer of poly(acrylonitrile), were used for the preparation of AMs [12–21]. For developing AMs, chloromethyl groups were introduced via electrophilic-substitution reaction, followed by quaternization. Chloromethylation was achieved by chloromethyl ethers or dihalomethyl ethers. Thermally and chemically stable high performance polymers (polysulfone or PEEK) based AMs were also prepared by chloromethylation with chloromethyl ether or chloromethyl–octylether, respectively [22,23]. In these methods, preparation of AMs was achieved by chloromethylation using chloromethyl ether (CME) followed by amination with a tertiary amine. In chloromethylation, the CME used is carcinogenic and potentially harmful to human health [14,24]. Also, chloromethylation of poly(sulfone) has been reported by mixture of paraformaldehyde, trimethylchlorosilane and a Lewis acid ($SnCl_4$) [25]. But, no attention was rendered to achieve the chloromethylation of PEEK using non-hazardous chemicals.

PEEK is insoluble in organic solvents, thus its partial sulphonation seems to be suitable option to achieve the high degree of chloromethylation. But, extra care should be necessary to control the degree of sulfonation and further complete replacement of $-SO_3H$ with $-CH_2Cl$ groups to avoid zwitterionic properties. By varying the reaction time, temperature, acid concentration and PEEK content, degree of sulfonation can be easily controlled [26–30]. Reported method avoids the use of hazardous and carcinogenic chemicals. Proposed reaction is diversified in nature and can be used for developing anion-exchange membranes or functionalized polymers.

2. Experimental section

2.1. Materials

Polyether ether ketone (PEEK, medium melt viscosity grade 450PF; Victrex PLC (England), stannic chloride, paraformaldehyde,

* Corresponding author. Tel.: +91 9925125760; fax: +91 278 2567562/6970.
E-mail addresses: vkshahi@csmcri.org, vinodshahi1@yahoo.com (V.K. Shahi).

0376-7388/$ - see front matter © 2012 Elsevier B.V. All rights reserved.
http://dx.doi.org/10.1016/j.memsci.2012.11.016

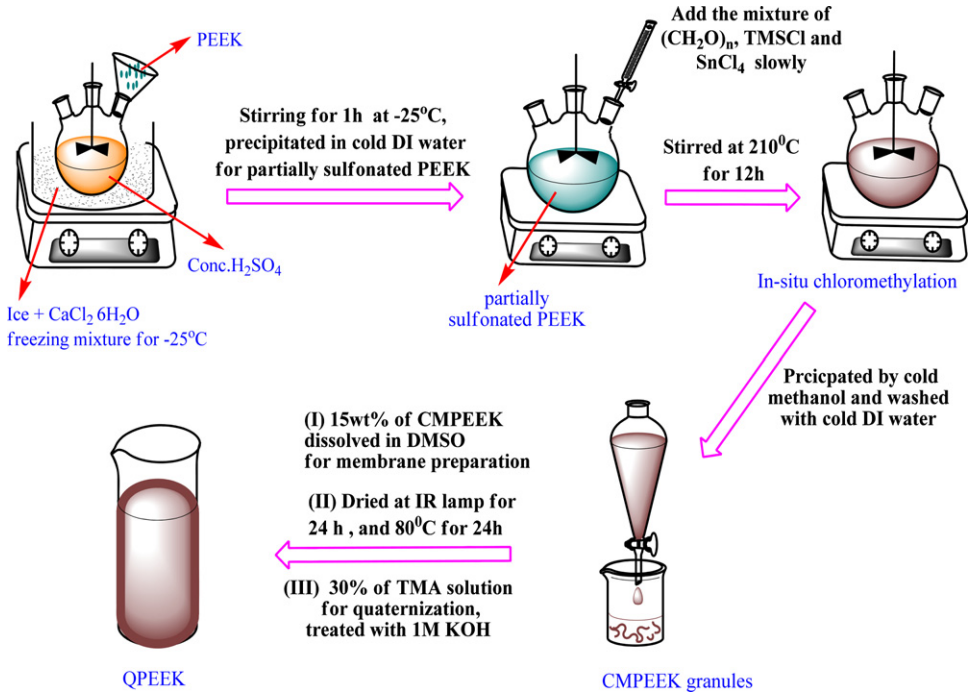

Fig. 1. Schematic presentation for CMPEEK and QPEEK synthesis.

trimethylsilylchloride (TMSCl), methanol, ethanol, sulphuric acid (98%), *N,N*-dimethylformamide (DMF), dimethyl acetamide (DMAc), dimethylsulfoxide (DMSO), *N*-methyl-2-pyrrolidone (NMP), and trimethylamine (TMA) (AR grade; SD Fine Chemicals, India) were used as received. Distilled deionized water was used for all experiments.

2.1.1. Synthesis of CMPEEK

Synthesis procedure for CMPEEK has been depicted in Fig. 1. PEEK was dissolved in conc. H_2SO_4 (20 wt%) in a cooling bath at −25 °C temperature for 1 h. Reaction was achieved at extremely low temperature for controlling the degree of sulfonation in precise manner. The reaction mixture was precipitated in cooled water, to obtain partially sulfonated PEEK. The partially sulfonated PEEK was dissolved in a NMP (10 wt%), in-situ chloromethylation was carried out by using paraformaldehyde, TMSCl and $SnCl_4$ at 210 °C under stirred condition for 12 h. Reaction mixture was precipitated in chilled methanol to obtain final product (CMPEEK), followed by washing in cold water to remove impurities.

2.1.2. Preparation of AMs

Synthesized CMPEEK was dissolved in DMSO (15 wt%) to cast thin film of desired thickness onto a cleaned glass plate (Fig. 2). Obtained thin film was dried under IR lamp for 24 h and aminated with TMA solution (30%) for 24 h. These alkaline membranes were further treated with 1 M KOH solution for 24 h. Conditioned membrane was subjected for physicochemical and electrochemical characterization. Prepared AMs were designated as QPEEK-*X*, where *X* is the degree of chloromethylation (%).

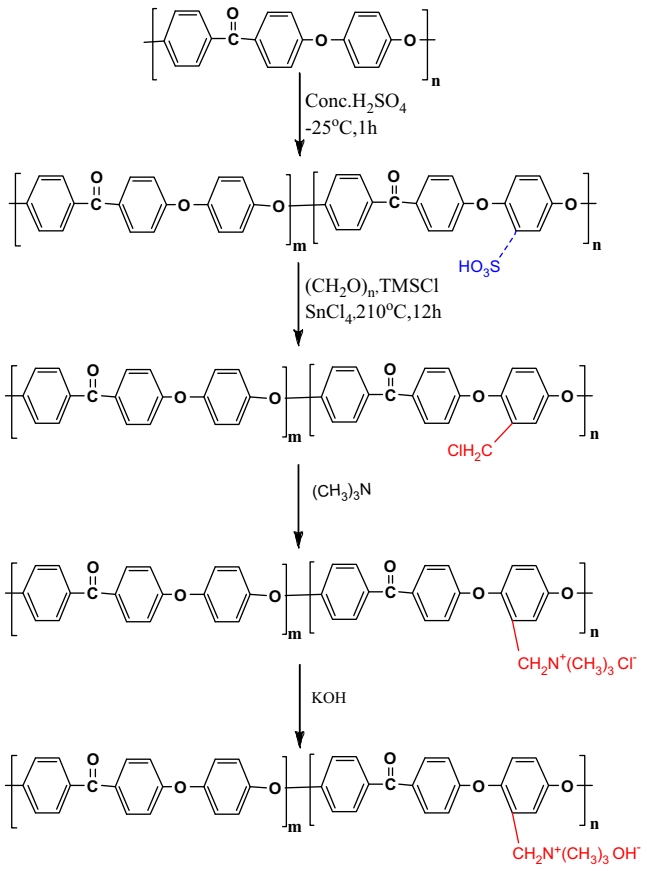

Fig. 2. Schematic presentation for the synthesis of QPEEK-OH.

2.2. Instrumental characterizations

The ^1H NMR, ^{13}C CP/MAS (cross polarization/magic angle spinning) spectrum of chloromethylated PEEK was recorded by NMR spectrometer (Bruker, 200 MHz for ^1H NMR and 125 MHz for CP/MAS), Fourier transform infrared (FTIR) spectra were recorded with spectrum GX series 49387 by ATR techniques. The elemental analysis (CHNS) was carried out using Perkin-Elmer-2400 CHNS analyzer for the percentage composition of the elements. Scanning electron microscopy (SEM) images of the

dried membranes were recorded by LEO Instruments (Kowloon, Hong Kong) microscope after the gold sputter coatings on membrane samples. Thermal analysis was carried out by thermogravimetric analyzer (TGA) (Mettler Toledo TGA/SDTA851^e with star^c software) under nitrogen atmosphere at 10 °C/min heating rate (50–600 °C). Differential scanning calorimetry (DSC) (Mettler Toledo DSC822^e) measurements were also performed between −30 and 30 °C.

2.2.1. Membrane characterizations and stabilities

Detailed procedure adopted for membrane conductivity, solvent uptake, ion exchange capacity (IEC), surface charge concentration and electro-osmotic permeability, have been included in Section S1 [31]. Membrane stabilities under harsh oxidative, hot aqueous and acidic environments were assessed by long-term aging experiments in respective mediums. Oxidative stability served as an accelerated test to simulate the strong oxidative water splitting conditions and membrane degradation by oxy active radicals [31,32]. Oxidative stability of QPEEK membrane was evaluated in Fenton's reagent at 80 °C for a specific time period. Membrane hydrolytic stability was assessed under boiled water condition (100 °C) for 24 h in a pressurized closed vial. Membrane alkaline stability was assessed by treating it in 10 M KOH for 24 h at 100 °C. Membrane stabilities were evaluated by loss in weight, IEC, and conductivity of samples [33].

2.2.2. Estimation of hydroxide mobility and activation energy

Membrane conductivity data was used with advantage of estimation of hydroxide ion mobility ($\mu_{OH}-$) in the membrane phase:

$$\mu_{OH^-} = \frac{\sigma}{FX^m} \quad (1)$$

where F is the Faraday constant.

Membrane conductivity data at different temperatures under 100% relative humidity (RH) (Fig. S5) was used for the estimation of activation energy (E_a) by following expression:

$$E_a = -b \times R \quad (2)$$

where b is the slope of the regression line of ln σ (S cm^{-1}) vs. 1000 T^{-1} (K^{-1}) plot and R is the gas constant (8.314 J K^{-1} mol^{-1}).

2.2.3. Chronopotentiometry and methanol permeability measurements

Chronopotentiometry responses of AMs were recorded in dilute NaCl solution using a two-compartment Perspex cell separated by a membrane (25 cm^2) (Fig. S1). Detailed procedure has been included in Section S2. Detailed procedure for methanol permeability and counter ion transport number measurements has been included in Section S3 and S4.

2.2.4. Preparation of membrane electrode assembly (MEA) and fuel cell testing

Membrane electrode assembly with three-layer structure (QPEEK-75, anode/cathode catalyst layer (Pt/C, 40 wt%) and diffusion layers) were prepared. It was a three-step preparation consisting of (i) wet proofing of carbon paper (Toray Carbon Paper, thickness: 0.27 mm), (ii) coating of a gas diffusion layer (GDL) onto the carbon paper, and (iii) coating of a catalyst layer onto the GDL. The carbon paper was wet proofed with 15 wt% PTFE solution by the brush painting method. The GDL (25 cm^2 geometric area) was fabricated by coating slurry of 0.50 mg/cm^2 consisting of carbon black (Vulcan XC72R) and PTFE dispersion on carbon paper. The Pt loading in both the anode and cathode was 4 mg/cm^2 in 5 wt% QPEEK ionomer solution. Thus, the obtained electrode was cold pressed membrane followed by curing at 60 °C for 12 h and then hot pressed at 130 °C for 3 min at 1.2 MPa. The MEA was achieved by hot pressing an electrode/membrane/electrode sandwich at a temperature of 100 °C for 3 min at 1.0 MPa. The MEA was assembled into a single cell (FC25-01 DM fuel cell). H_2 at anode and air at the cathode were fed with 50 ml min^{-1}, and 100 ml min^{-1}, respectively, to record the current–voltage polarization curves with the help of an MTS-150 manual fuel cell test station (ElectroChem Inc., USA). Single cell performance was performed at 50 °C with 100% relative humidity for QPEEK-75 membrane.

3. Results and discussion

3.1. Preparation of AMs

PEEK was dissolved in conc. H_2SO_4 at a temperature of −25 °C and degree of sulfonation was estimated by ^{1}H NMR and CHNS analysis. The partially sulfonated PEEK was dissolved in NMP at 210 °C, to achieve the desulphonation [34–37]. In-situ chloromethylation was carried out in presence of $(CH_2O)_n$, TMSCl and $SnCl_4$, under stirred condition for 12 h. Reaction mixture was cooled and CMPEEK was precipitated in chilled methanol. The possible mechanism has been presented in Scheme 1. The presence of –CH_2Cl group was confirmed by ^{1}H NMR and ^{13}C CP/MAS NMR (Fig. 3). In the first step, partially sulphonated PEEK was formed and characterized by ^{1}H NMR. Degree of sulfonation (DS) was estimated about 10% (Fig. 3a) [38].

In second step, chloromethylation was confirmed and estimated by ^{1}H NMR and ^{13}C CP–MAS spectrum (Fig. 3(b–e)). ^{1}H NMR showed –CH_2Cl peak at 4.581 ppm, while ^{13}C CP/MAS spectrum showed peak at 47.89 ppm. The degree of chloromethylation (DCM) was estimated by using ^{1}H NMR through the Eq. (3) [23].

$$\mathrm{DCM} = \frac{2A(H_d)}{A(H_c)} \quad (3)$$

where A (H_d) is the integral area of the H_d peak (–CH_2Cl), and A (H_c) is the one of the H_c peak. Designated peak values are included

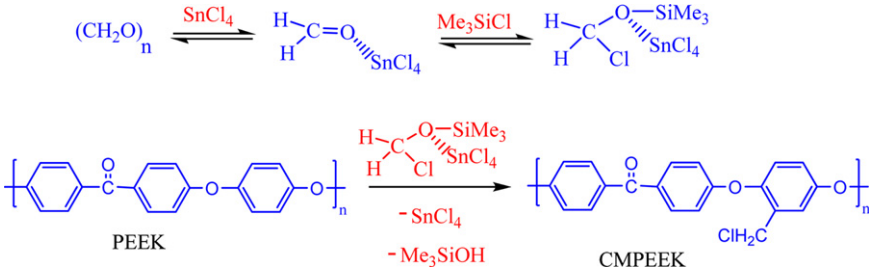

Scheme 1. Proposed mechanism for in-situ chloromethylation of PEEK.

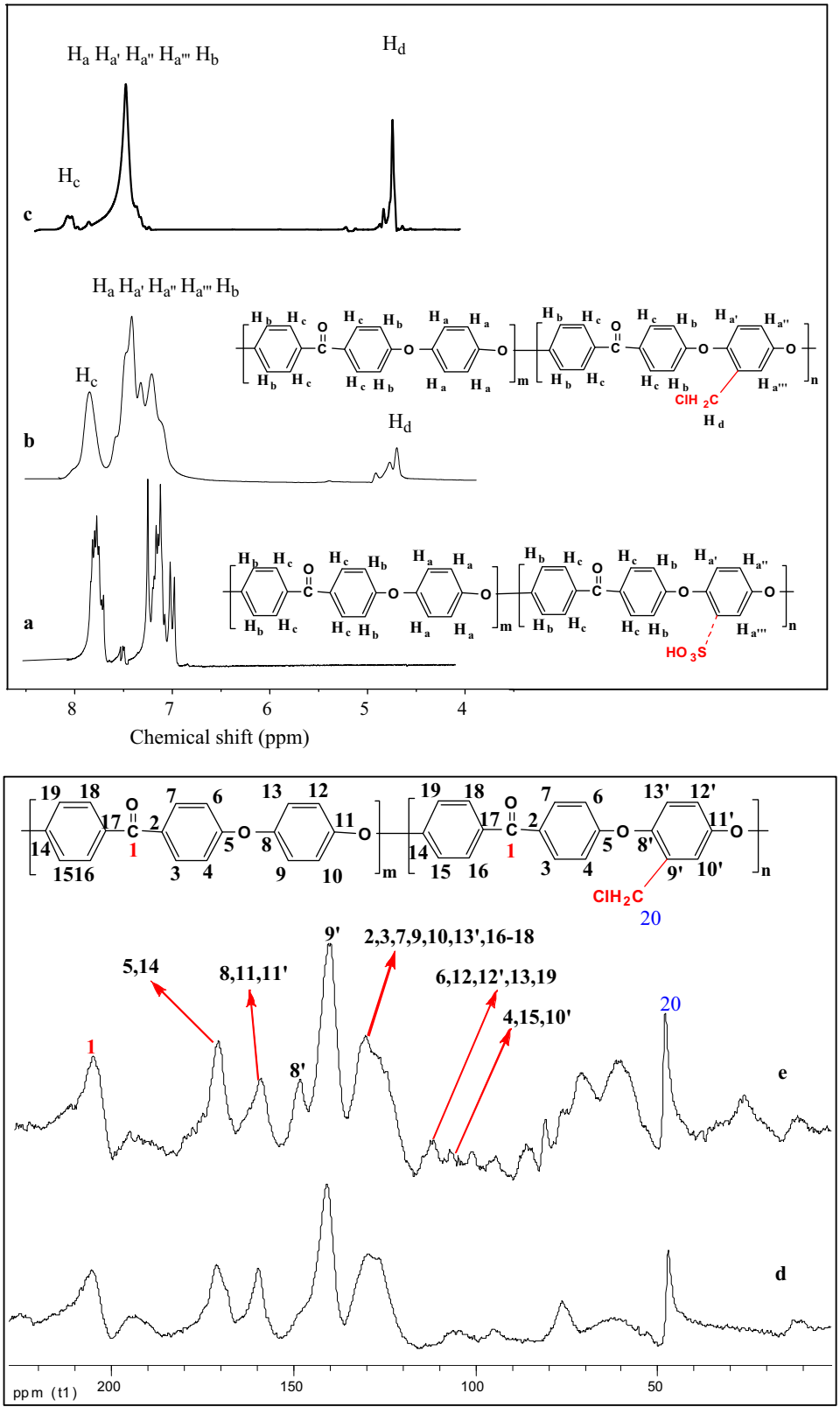

Fig. 3. ^{1}H NMR spectrum of: (a) partially sulfonated PEEK-10, (b) CMPEEK-35, (c) CMPEEK-75 and ^{13}C CP/MAS NMR Spectrum of: (d) CMPEEK-35, (e) CMPEEK-75.

in Tables-1a and b, while DCM values for different AMs are included in Table 3. ^{1}H NMR spectra confirmed absence of sulphonic acid groups and complete desulphonation for CMPEEK-35, CMPEEK-75, (Fig. 3b and c).

Chloromethylation of PEEK was also confirmed by FTIR spectra (Fig. 4). The peak at 3030–3070 cm^{-1} (C–H), and 1500–1600 cm^{-1} (C=C) were aroused due to aromatic ring of PEEK. The C=O band showed at 1660 and 3420 cm^{-1}, while bands at

Table 1 (a)
Chemical shift values of ^{1}H NMR spectrum of SPEEK-10, CMPEEK-35 and CMPEEK-75.

SPEEK-10		CMPEEK-35		CMPEEK-75	
δ(ppm)	^{1}H designation	δ(ppm)	^{1}H designation	δ(ppm)	^{1}H designation
7.01–7.26	H_a, $H_{a'}$, $H_{a''}$, H_b	7.20–7.46	H_a, $H_{a'}$, $H_{a''}$, $H_{a'''}$, H_b	7.07–7.22	H_a, $H_{a'}$, $H_{a''}$, $H_{a'''}$, H_b
7.73–7.81	H_c	7.77	H_c	7.77–7.78	H_c
7.57	$H_{a'''}$	4.582	H_d	4.589	H_d

Table 1 (b)
Chemical shift values of ^{13}C MAS spectrum of CMPEEK-35 and CMPEEK-75.

CMPEEK-35 δ(ppm)	^{13}C designation	CMPEEK-75 δ(ppm)	^{13}C designation
47.15	20	47.89	20
104–110	4, 15	104.4–107.16	4, 15,
104–110	10'	111–112	10'
124–126	6, 12, 13, 19	124–130	6, 10, 12, 13, 19
126–130	12′	124–130	12′
126–130	10, 13′	124–130	13′
126–130	2, 3, 7, 9, 16–18	124–130	2, 3, 7, 9, 16–18
140	9′, 8'	140	9′
159	11′	148	8′, 11′
159	8, 11	159	8, 11
171	5, 14	171	5, 14
205	1	205	1

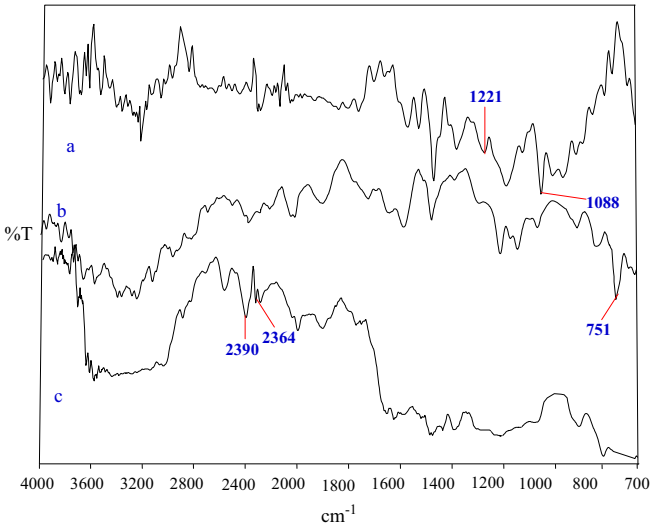

Fig. 4. FTIR spectrum for: (a) partial sulfonated PEEK, (b) CPEEK and (c) QPEEK.

1240 cm^{-1} were assigned to anti-symmetric vibration of aromatic ether group. SPEEK membrane showed the band at 1088 and 1221 cm^{-1} assigned for S=O bond of sulphonic acid group (Fig. 4a) [39]. In Fig. 4b, characteristic bands at 751 cm^{-1} confirmed C–Cl bond of chloromethylation (CMPEEK) [40]. The characteristics bands of quaternary ammonium groups appeared 2364 and 2390 cm^{-1} (Fig. 4c) [40,41].

SEM images of QPEEK-75 membrane in alkaline state exhibited uniform and compact membrane surface without any pore or cavity (Fig. S2). DS and degree of quaternization were also studied by CHNS analysis (Table S1) [38].

3.2. Membrane stabilities

Thermogravimetric analysis (TGA) for QPEEK-75 membrane exhibited weight loss below 100 °C due to evaporation of absorbed water (Fig. S3). The second weight loss (320 °C) was attributed to degradation residual groups (e.g., $–CH_2OH$ and $–CH_2N(CH_3)_2$) and quaternary ammonium groups. Weight loss (%) linearly depended on DCM (Fig. S3). These results confirm thermal stability of QPEEK membranes beyond the range of interest for AMFCs.

Table 2
Alkaline stability in terms of loss in weight, ion-exchange capacity (IEC), and membrane conductivity (σ) for developed membranes.

Membrane	Alkaline stability (%)		
	W_{loss}	IEC_{loss}	σ_{loss}
QPEEK-75	12.15	16.16	16.39
QPEEK-48	11.94	13.97	14.11
QPEEK-35	11.40	12. 67	13.59

There is possibility of formation of H_2O_2 due to further reduction of OH^-, which may lead to the formation of $^{\bullet}OH$, and $^{\bullet}OOH$ radicals, responsible for chain scission of the polymer electrolyte [31,32]. Further, these free radicals are believed to be attack on hydrogen containing bonds of AMs. Membrane oxidative stability was evaluated by recording loss in weight, IEC and conductivity, after treatment with Fenton reagents (Fe^{2+}–H_2O_2) for 1 h at 80 °C (Table S2). In proximity of hydrophilic domains, per-oxy radical attacks aggressively at high temperature [31]. Further, deterioration in membrane properties (weight, IEC and conductivity) was enhanced (5–13%) with DCM. Data indicate that free radical attacked mainly on the polymer backbone rather than vicinity of hydrophilic domains. Furthermore, prepared membranes exhibited good oxidative stability. Accelerated hydrolytic stability test for prepared membranes was performed at 100 °C and 100% RH for 24 h. Membranes exhibited about 1.0–6.0% loss in weight, IEC and conductivity (Table S2). Also membranes subjected for test maintained their transparency, flexibility and toughness.

Alkaline stability of QPEEK membrane was assessed in 10.0 M KOH for 24 h at 100 °C (Table 2). About 11–17%, loss in weight, IEC and conductivity were attributed to alkaline tolerant polymer backbone in the absence of aliphatic beta H-atom around the quaternary ammonia group. This attractive feature of membrane avoids the Hoffmann degradation reaction and thus loss in membrane functional nature [42].

3.2.1. IEC, water uptake and state of water

IEC may be defined as the number of exchangeable functional groups per unit dry weight of membrane, and IEC values for QPEEK membranes (0.70–1.15 meq. g^{-1}) increased with DCM (Table 3). Water uptake values (*WU*) were also increased with DCM due to increase in hydrophilic groups in the membrane matrix. IEC along with *WU* values may be used with advantages for the estimation of net surface charge concentration (χ^m) (Table 3). An increase in χ^m values with DCM of PEEK, evidenced the enhanced membrane functional nature with increase in DCM.

Membrane performance in AMFCs depends on presence of water in the membrane matrix (responsible for hydroxide

Table 3
Degree of chloromethylation (%), water uptake (*WU*), water–methanol uptake (Φ_{w+MeOH}), ion-exchange capacity (IEC), surface charge concentration (X^m), electro-osmotic flux (J_e) and counter ion transport number (t_-^m) for different membranes.

Membranes	DCM (%)	IEC (meq g^{-1})	$X^m \times 10^{-3}$ (mol dm^{-3})	*WU (%)*	Φ_{w+MeOH}(%)	$J_e \times 10^{-8}$(ml C^{-1})	t_m
QPEEK-35	35	0.70	0.399	10.2	11.5	0.571	0.75
QPEEK-48	48	0.81	0.589	20.5	16.2	0.710	0.87
QPEEK-75	75	1.15	0.738	28.7	16.7	0.849	0.91

Table 4
Alkaline conductivity (σ), hydroxide mobility (μ_{OH}), iso-concentration (C_{iso}), iso-conductance (σ_{iso}), energy of activation (E_a) and methanol permeability (P) values for different membranes.

Membrane	$\sigma \times 10^{-3}$ (S cm^{-1})	$\mu_{OH-} \times 10^{-3}$ (cm^2 s^{-1} V^{-1})	C_{iso}(M)	$\sigma_{iso} \times 10^{-3}$ (S cm^{-1})	E_a (kJ mol^{-1})	$P \times 10^{-8}$ (cm^2 s^{-1})	
						30 (%)	50 (%)
QPEEK-35	16.0	0.416	0.085	15.13	23.1	3.44	8.11
QPEEK-48	17.5	0.455	0.090	16.56	20.5	4.98	9.88
QPEEK-75	20.0	0.519	0.092	19.13	16.7	5.39	18.92

conductivity) at high temperature. Total water present in the membrane matrix may be classified as [31]: (i) free water (with same temperature and enthalpy of melting as bulk water); (ii) freezing bound water (weakly bound with polar or ionic groups of polymer and shows a change in temperature and enthalpy in comparison with bulk water and can be detected by DSC); and (iii) non-freezing water (very strong interaction with polar or ionic groups and shows no phase transition). State of water can be determined by its association with hydrophilic domains. DSC melting thermograms (−30 to +30 °C) for different QPEEK membranes were used to elucidate the state of water in the membrane phase (Fig. S4). Thermograms showed a broad endothermic peak with two major melting peaks. The enthalpy of melting (ΔH_m), melting temperature (T_m), and full width at half-maximum of the melting peak (ΔT_m) for different QPEEK membranes were determined by the method reported earlier (Table S3) [31]. Increase in ΔH_m and ΔT_m values with DCM for QPEEK membrane, may be attributed to enhanced bound water percentage in the membrane matrix (necessary for solvation).

Number of free water molecule per ionic site (λ_f) in the wet membrane was obtained from the total melting enthalpy (peak area integration of the melting curves) (Fig. S4). Number of bound water molecules per ionic sites (λ_b) was estimated by subtracting the number of freezing water molecules from total number of water molecules per ionic sites. Percentage of bound water ($\chi = \lambda_b/\lambda_f$) was estimated from the ratio of bound water molecules per ionic sites to the total water molecules per ionic sites. Estimated values of λ_f, λ_b, and χ for different membranes are also included in (Table S3). With the increase in DCM of membrane matrix (quaternization), number of free water molecules in the membrane matrix decreased, while number of bound water increased, because availability of hydrophilic groups. Thus, reported QPEEK membrane exhibited high bound water content, necessary for hydroxide conductivity at elevated temperature.

3.2.2. Hydroxide ion conductivity and mobility

Hydroxide ion conductivity (σ) values for different QPEEK membranes have been included in Table 4. QPEEK-75 membrane exhibited 20.0 mS cm^{-1} conductivity in equilibration with 0.1 M NaOH solution. Further, membrane conductivity increased with concentration of equilibrating alkaline solutions and attended limiting value (Fig. 5). At low external concentration, pore solution conductivity (responsible for membrane conductivity) was high in compare with bulk solution, may be due high ionic

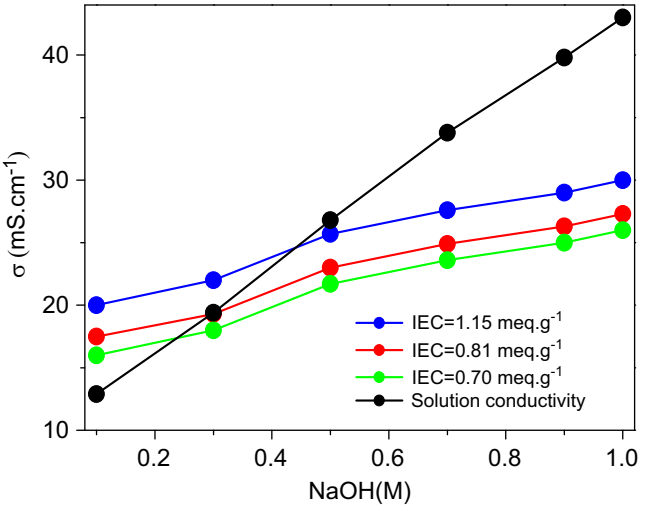

Fig. 5. Variation of membrane conductivity in equilibration of NaOH solutions of different concentrations.

molality in the membrane matrix. Initially conductivity increased rapidly with external solution concentration, afterwards increment was slow, until the concentration equilibrium of external and pore solutions [43]. Membrane conductivity also increased with the degree of quaternization in the membrane matrix (Table 4). The increase in σ value with degree of quaternization in the membrane matrix may be attributed to: (i) an increase in membrane IEC and water uptake; (ii) enhanced basic domain due to hydrophilic $-N^+(CH_3)_3$ functional groups for OH^- migration. It seems that these factors were mainly responsible for increase in membrane conductivity. Also, ΔH_m depends on the free water content in the membrane matrix. Thus, high extent of free water in the membrane matrix is essential for easy conduction of OH^- through the membrane. Membrane conductivity observations reveal the necessity for designing an AM with high extent of free water in the membrane matrix suitable for an electrochemical process. Membrane conductivity for QPEEK-75 was compared with other AMs reported in the literature (Table 5) [44–48].

Gnusin [49] and Zabolotsky and Nikonenko [50] proposed model, in which an IEM was considered as a combination of gel phase and integral phase with volume fractions f_1 and f_2, respectively, ($f_1+f_2=1$). The integral phase represents the inner parts of meso/microspores (voids/cavities), while the gel phase represents

electro neutral nanoporous medium, consisting of fixed and mobile ions, water and polymer matrix [51]. The micro heterogeneous structure of the membrane matrix is mainly responsible for the concentration-dependent properties such as conductivity, diffusion permeability, and counter-ion transport [52]. Considering micro heterogeneous nature of AM, membrane conductivity may be expressed as: [53]

$$\log\sigma = f_1 \log\sigma_{iso} + f_2 \log\sigma_s \quad (4)$$

where σ_{iso} is the conductivity at the iso-conducting point, and σ_s is the solution conductivity. The σ_{iso} and iso-concentration (C_{iso}) values were estimated from intercept of σ vs. σ_s curves (Fig. 5), and increased with degree of quaternization. These values predict the concentration range over which the membranes will be most efficient in the various electrochemical processes. Further, the f_1 and f_2 values were calculated from the log σ vs. log σ_s plot (Table 4). Low f_2 values imply the less fraction of the non-conducting region in the membrane matrix. In this case, f_1 value revealed that the volume fraction of conducting gel phase increased, while volume fraction of non-conducting phase (f_2) decreased with increase in degree of quaternization in the membrane matrix.

Hydroxide ion conductivity (σ) in the membrane phase is highly dependent on ionic mobility and fixed charge concentration in the membrane matrix. The $\mu_{OH}-$ values for different membranes ranged between 0.410 and 0.519 $\times 10^{-3}$ cm^2 s^{-1} V^{-1} (Table 4). Hydroxide ion mobility in the membrane phase increased with the degree of quaternization, may be due to enhanced hydration and conducting channels and clusters in the membrane matrix. $\mu_{OH}-$ values were dependent on IEC values and increased with degree of quaternization in the membrane matrix. A higher value of the free water content assists proton conduction by reducing the tortuous path and resistance for the proton within the membrane matrix. Further, the $\mu_{OH}-$ value for QPEEK-75 membrane confirmed easy hydroxide ion conduction process across it.

Table 5
Comparison of membrane conductivity for QPEEK-75 and other AMs reported in the literature.

Membrane	$\sigma \times 10^{-3}$ (S cm^{-1})	Ref.
SEBS[a]	9.37(80 °C)	44
Cardo polyetherketone[b]	5.06 (60 °C)	45
QAPEEKOH [c]	12 (30 °C)	23
Poly(MMA-*co*-BA-*co*-VBC)[d]	5.2–13.5(80 °C)	46
PVA/silica[e]	8, (25 °C)	47
Cross-linked QPVA[f]	7.34, (30 °C)	48
QPEEK [g]	14.63, (30 °C)	This work

SEBS.

[a] = Polystyrene-block-poly(ethylene-ran-butylene)-block-polystyrene.
[b] = Quaternized cardo polyetherketone anion exchange membrane.
[c] = quaternized PEEK hydroxidemembrane. Poly(MMA-co-BA-co-VBC).
[d] =Quaternized poly(methyl methacrylate-*co*-butyl acrylate-*co*-vinylbenzyl chloride), PVA/silica.
[e] =Poly(vinyl alcohol)/3-(trimethylammonium) propyl-functionalized silica hybrid membrane, Cross-linked QPVA.
[f] =cross-linked quaternized poly(vinyl alcohol) membranes, QPEEK.
[g] =Quaternized poly(ether ether ketone).

Membranes showed positive temperature-conductivity dependencies, which suggest thermal activated conduction process (Table 4). E_a values (16.2–23.1 kJ mol^{-1}) increased with the degree of quaternization, and was higher than that in compare with Nafion 117 membrane (6.52 kJ mol^{-1}) [5]. Furthermore, high E_a values of QPEEK membranes at elevated temperature indicate it followed Grotthus-type conduction mechanism. Inter-linked and continuous hydrophilic channels were responsible for fast ion/molecule diffusion and rapid conduction, at high temperature.

3.3. Chronopotentiometry

Membrane homogeneity was predicted by chronopotentiometry studies using following Eq. [54]

$$\tau = \left(\frac{nFC}{2(t_i^m - t_i)}\right)^2 \times \frac{(D\pi)}{i^2} \quad (5)$$

where D is the diffusion coefficient of the electrolyte, $t_i^m$the counter-ion transport number in the membrane phase, t_i the counter-ion transport number in the solution phase, τ the transition time, C_i concentration of the electrolyte, F the faraday constant, and i the applied current density. Typical shape of chronopotentiometry curve (in equilibration with 0.1 M NaOH solution at 24.0 mA cm^{-2} applied constant current density) for QPEEK membrane revealed its homogeneous nature (Fig. 6A) [55–57]. Initial potential (point a) aroused due to the Ohmic resistance of membrane–solution interface. Inflection (point b) was observed due to depletion of counter-ion (OH^-) by electro-diffusion processes causing concentration polarization. Section 1 corresponds to the potential growth, while beyond inflection point (Section 2); potential was governed by mass transfer mechanism (convection). Inflection was observed only due to high applied current density in compare with limiting current density. In case of low applied current density, transport occurs through electro-diffusion, and no inflection was observed

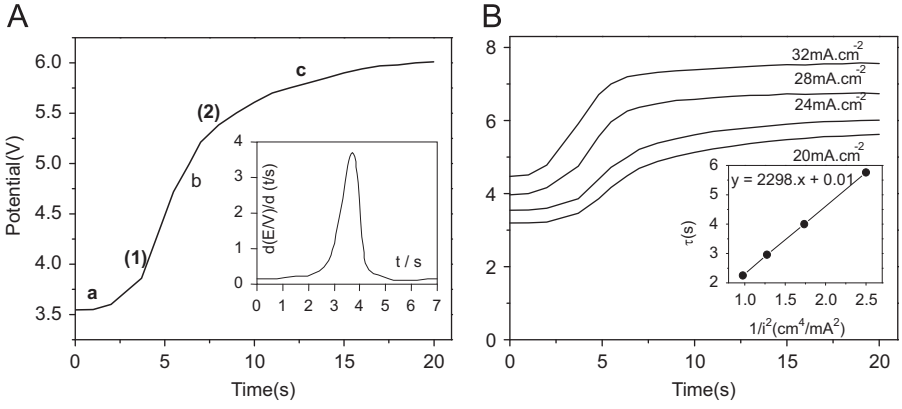

Fig. 6. (A) Chronopotentiometric curve for alkaline QPEEK membrane and its derivative in 0.1 M NaCl solution at 24 mA cm^{-2} applied current density and (B) chronopotentiometric curves of the alkaline QPEEK membrane in 0.1 M NaCl solution at different current densities.

[55,58,59]. The transition time corresponds to the maximum point of the derivative curve (insert Fig. 6A). For a given electrolyte concentration, τ linearly depends on $1/i^2$ (Fig. 6B). Earlier reported AM (CMS, CMV, ASV and AMX) did not showed sufficient homogeneity because of binder (poly(vinyl chloride) [60,61]. QPEEK membranes showed well defined chronopotentiograms and thus homogeneous in nature as also revealed by SEM analysis (Fig. S2).

Based on Eq. (5), diffusion coefficient for OH^- was determined by estimating t_i^m values by Hittorf's method (0.870). Estimated value of diffusion coefficient of OH^- (1.61×10^{-5} $cm^2\ s^{-1}$) is very close to the values reported in the literature (1.48×10^{-5} $cm^2\ s^{-1}$) [62]. This also confirms hydroxide selective nature of QPEEK membranes.

3.4. Electro-osmotic permeability

In fuel cell, methanol (fuel) cross-over occurred through electro-osmotic drag across membrane. Thus, study on electro-osmotic permeability of QPEEK membrane is essential for better understanding for fuel cross-over and intelligent designing of membranes. Electro-osmotic flux across the ion exchange membranes was aroused due to: (i) the presence of charged sites on the membrane matrix and (ii) the existence of an electrical potential at the membrane solution interface called zeta potential. The electro-osmotic permeability of different QPEEK membranes in equilibration with 0.01 M NaOH solution varied between 0.571 and 0.849×10^{-8} $cm^3\ C^{-1}$ increased with degree of quaternization of the membrane matrix (Table 3). High density of quaternary ammonium groups (exchangeable charged groups) in the membrane matrix was responsible for increase in electro-osmotic drag.

3.5. Methanol permeability and selectivity parameter

Water–methanol uptake (Φ_{w+MeOH}) values for different membrane are presented in Table 3. Φ_{w+MeOH} values are increased with quaternized content because membrane hydrophilic groups interact with methanol via intermolecular H-bonding and allow absorption of large quantity of methanol in the membrane matrix. Thus, moderate quaternized content of QPEEK membrane was suitable for fuel cell application. QPEEK membranes exhibited significantly low methanol permeability in compare with Nafion117 membrane at 30% v/v water–methanol mixture (Table 4). The methanol permeability and selectivity parameter for different AMs have been included in Section S3.

3.6. Fuel cell for QPEEK-75 membrane

The QPEEK-75 membrane behaved as strong alkaline electrolyte (1.15 meq g^{-1}). Membrane in OH^- form was used for MEA preparation. Presence of Cl^- could result in the deactivation of catalyst; therefore Cl^- was fully exchanged. The fuel cell performance was observed in the absence of any liquid electrolyte. Fig. 7 shows the current–voltage polarization curve of the cell with QPEEK-75 membrane at 50 °C with 100% relative humidity and ambient pressure. Open circuit voltage (OCV) of the H_2/air fuel cell was 1.02 V. High OCV was obtained due to low permeation of reactant gaseous through the membrane and favourable electrochemical reaction kinetics in alkaline medium. Peak power density (48 mW cm^{-2}) was obtained at 109 mA cm^{-2} current density. Cell voltage decreased gradually with current density. Cell behaviour was affected by surface activity of electrode and membrane-electrode interfacial property played significant role. We have not paid much attention to optimize the AMFC conditions, because objective of the work was to achieve high degree of chloromethylation of PEEK for developing alkaline membrane

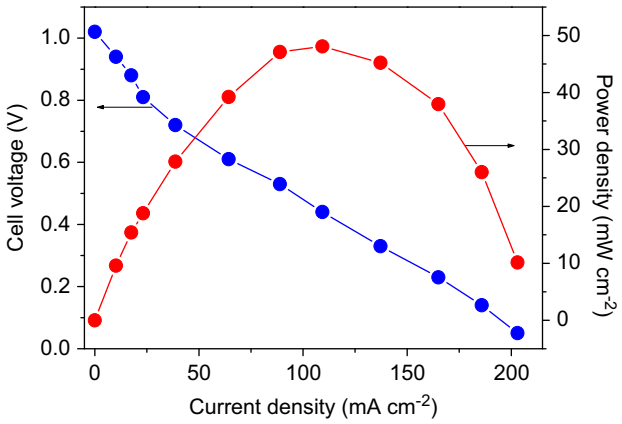

Fig. 7. Fuel cell performance of QPEEK-75 under 100% humidity at 50 °C.

4. Conclusions

PEEK was partially sulfonate to enhance its solubility followed by chloromethylated with paraformaldehyde and chlorotrimethylsilane in the presence of Lewis acid catalyst. Quaternization was carried out for developing AMs. Instrumental analysis evidenced complete replacement of $–SO_3H$ with $–CH_2Cl$ groups. Proposed method for chloromethylation avoids the use of carcinogenic and hazardous chemicals. Desired properties of AMs were achieved by controllable DCM (estimated from NMR studies and found to be varied between 35 and 75%). QPEEK membranes showed good thermal, oxidative and alkaline stabilities, avoids Hoffmann degradation and thus deterioration in membrane functional nature. Prepared membranes showed good physiochemical and electrochemical properties along with well defined chronopotentiograms, which revealed their homogeneous and strong alkaline nature. Alkaline conductivity of QPEEK membrane (especially QPEEK-75) was higher than reported alkaline membranes in the literature, and its high E_a values confirmed Grotthus-type of OH^- conduction mechanism, because of continuous and inter-linked hydrophilic channels. About 1.02 V OCV and 48.09 mW cm^{-2} peak power density at 109.3 mA cm^{-2} current density in H_2/air were obtained under fuel cell testing conditions. Testing results exhibited promising performance of AMFC with QPEEK-75 membrane developed in this study. These results demonstrated the grate prospect of QPPEK membranes and preparation route for AMFC applications. Furthermore, reported, reaction also can be used for functionalization of aromatic polymers for developing anion-exchange membrane or other membrane based devices.

Acknowledgements

Financial assistance received from the Ministry of New and Renewable Energy (MNRE), Government of India, is gratefully acknowledged for sponsoring project no. 102/79/2010-NT. We also acknowledge the Analytical Science Division, CSMCRI, Bhavnagar for instrumental support.

Appendix A. Supporting information

Supplementary data associated with this article can be found in the online version at http://dx.doi.org/10.1016/j.memsci.2012.11.016.

Nomenclature

WU	water uptake
Φ_{w+MeOH}	water–methanol uptake
X^m	surface charge concentration (mol dm^{-3})
J_e	electro-osmotic flux (ml C^{-1})
t_-^m	counter ion transport number
σ	membrane conductivity (mS cm^{-1})
σ_s	solution conductivity (mS cm^{-1})
μ_{OH-}	hydroxide ion mobility (cm^2 s^{-1} V^{-1})
C_{iso}	iso-concentration (M)
σ_{iso}	membrane iso-conductance (S cm^{-1})
f_1	gel phase volume fractions
f_2	integral phase volume fractions
E_a	energy of activation (kJ mol^{-1})
R	gas constant (J K^{-1} mol^{-1})
T	absolute temperature (K)
P	methanol permeability (cm^2 s^{-1})
δ	chemical shift (ppm)
ΔH_m	enthalpy of melting (J/g)
T_m	melting temperature (°C)
ΔT_m	full width at half-maximum of the melting peak (°C)
λ_t	total number of water molecules per ionic site
λ_b	number of bound water molecules per ionic site
χ^b	degree of bound water
A	effective membrane area (m^2)
l	membrane thickness (cm)
F	Faraday constant
I	applied current density (mA cm^{-2})
t	time (s)
E	applied potential (V)
V	total volume (cm^3)
ρ_d	membrane density
Δx	membrane thickness (cm)
R^m	membrane resistance (Ω)
φ_w	volume fraction of water in membrane matrix
n	ion valency
D	diffusion coefficient (cm^2 s^{-1})
τ	transition time (s)

References

[1] M.A. Hickner, H. Ghassemi, Y.S. Kim, B.R. Einsla, J.E. McGrath, Alternative polymer systems for proton exchange membranes (PEMs), Chem. Rev. 104 (2004) 4587–4611.

[2] C.H. Park, C.H. Lee, M.D. Guiver, Y.M. Lee, Sulfonated hydrocarbon membranes for medium-temperature and low-humidity proton exchange membrane fuel cells (PEMFCs), Prog. Polym. Sci. 36 (2011) 1443–1498.

[3] T.J. Peckham, S. Holdcroft, Structure–morphology–property relationships of non-perfluorinated proton-conducting membranes, Adv. Mater. 22 (2010) 4667–4690.

[4] B.P. Tripathi, V.K. Shahi, Organic-inorganic nanocomposite polymer electrolyte membranes for fuel cell applications, Prog. Polym. Sci. 36 (2011) 945–979.

[5] B.P. Tripathi, V.K. Shahi, Functionalized organic–inorganic nanostructured *N*-*p*-carboxy benzyl chitosan-silica-PVA hybrid polyelectrolyte complex as proton exchange membrane for dmfc applications, J. Phys. Chem. B 112 (2008) 15678–15690.

[6] J.R Vorcoe, R.C.T. Slade, Prospects for alkaline anion-exchange membranes in low temperature fuel cells, Fuel Cells 5 (2005) 187–200.

[7] T. Xu, Ion exchange membranes: state of their development and perspective, J. Membr. Sci. 263 (2005) 1–29.

[8] M.A. Hickner, Ion-containing polymers: new energy & clean water, Mater. Today 13 (2010) 34–41.

[9] (a) G. Merle, M. Wessling, K. Nijmeijer, Anion exchange membranes for alkaline fuel cells: a review, J. Membr. Sci. 377 (2011) 1–35;
(b) F. Zhang, H. Zhang, C. Qu, Imidazolium functionalized polysulfone anion exchange membrane for fuel cell application, J. Mater. Chem. 21 (2011) 12744–12752.

[10] N. Li, T. Yan, Z. Li, T.T. Albrecht, W.H. Binder, Comb-shaped polymers to enhance hydroxide transport in anion exchange membranes, Energy Environ. Sci. 5 (2012) 7888–7892.

[11] S. Zhang, T. Xu, C. Wu, Synthesis and characterizations of novel, positively charged hybrid membranes from poly(2,6-dimethyl-1,4-phenylene oxide), J. Membr. Sci. 269 (2006) 142–151.

[12] M.R. Hibbs, M.A. Hickner, T.M. Alam, S.K. McIntyre, C.H. Fujimoto, C.J. Cornelius, Transport properties of hydroxide proton conducting membranes, Chem. Mater. 20 (2008) 2566–2573.

[13] J.R. Varcoe, R.C.T. Slade, E.L.H. Yee, S.D. Poynton, D.J. Driscoll, D.C. Apperley, Poly(ethylene-*co*-tetrafluoroethylene)-derived radiation-grafted anion-exchange membrane with properties specifically tailored for application in metal-cation-free alkaline polymer electrolyte fuel cells, Chem. Mater. 19 (2007) 2686–2693.

[14] S. Singh, A. Jasti, M. Kumar, V.K. Shahi, A green method for the preparation of highly stable organic–inorganic hybrid anion-exchange membranes in aqueous media for electrochemical processes, Polym. Chem. 1 (2010) 1302–1312.

[15] M. Kumar, S. Singh, V.K. Shahi, Cross-linked poly(vinyl alcohol)–poly(acrylonitrile-*co*-2-dimethylamino ethylmethacrylate) based anion-exchange membranes in aqueous media, J. Phys. Chem. B 114 (2010) 198–206.

[16] J.R. Varcoe, R.C.T. Slade, E.L.H. Yee, An alkaline polymer electrochemical interface: a breakthro—ugh in application of alkaline anion-exchange membranes in fuel cells, Chem. Commun. (2006) 1428–1429.

[17] D. Stoica, F. Alloin, S. Marais, D. Langevin, C. Chappey, P. Judeinstein, Polyepichlorhydrin membranes for alkaline fuel cells: sorption conduction properties, J. Phys. Chem. B 112 (2008) 12338–12346.

[18] B. Tang, P. Wu, H.W. Siesler, Insitu study of diffusion interaction of water mono- or divalent anions in a positively charged membrane using two-dimensional correlation ft-ir/attenuated total reflection spectroscopy, J. Phys. Chem. B 112 (2008) 2880–2887.

[19] Y. Wu, C. Wu, T. Xu, Y. Fu, Novel anion-exchange organic–inorganic hybrid membranes prepared through sol–gel reaction of multi-alkoxy precursors, J. Membr. Sci. 329 (2009) 236–245.

[20] Y. Xiong, Q.L. Liu, Q.G. Zhang, A.M. Zhu, Synthesis characterization of cross-linked quaternized poly(vinyl alcohol)/chitosan composite anion exchange membranes for fuel cells, J. Power Sources 183 (2008) 447–453.

[21] M.R. Hibbs, C.H. Fujimoto, C.J. Corneli, Synthesis characterization of poly(phenylene)-based anion exchange membranes for alkaline fuel cells, Macromolecules 42 (2009) 8316–8321.

[22] G. Wang, Y. Weng, D. Chu, R. Chena, D. Xie, Developing a polysulfone-based alkaline anion exchange membrane for improved ionic conductivity, J. Membr. Sci. 332 (2009) 63–68.

[23] X. Yan, G. He, S. Gu, X. Wu, L. Du, H. Zhang, Quaternized poly(ether ether ketone) hydroxide exchange membranes for fuel cells, J. Membr.Sci. 375 (2011) 204–211.

[24] US Department of Health Human Services. Public Health Service, National Toxicology Program. Report on Carcinogens, Twelfth Edition. (2011) 〈http://ntp.niehs.nih.gov/ntp/roc/twelfth/roc12.pdf〉.

[25] E. Avram, E. Butuc, C. Luca, I. Druta, Polymers with pendant functional group. III. polysulfones containing viologen group, J. Macromol. Sci-Pure. Appl. Chem. A 34 (1997) 1701–1714.

[26] H.H. Ulrich, G. Rafler, Sulfonated polyaryl ether ketones, Die Angewte Makromolekulare Chemie 263 (1998) 71–78.

[27] R. Jiang, H.R. Kunz, J.M. Fenton, Investigation of membrane property and fuel cell behavior with sulfonated poly(ether ether ketone) electrolyte: temperature and relative humidity effects, J. Power Sources 150 (2005) 120–128.

[28] Y. Dai, X. Jian, X. Liu, M.D. Guiver, Synthesis and characterization of sulfonated poly(phthalazinone ether sulfone ketone) for ultrafiltration and nanofiltration membranes, J. Appl. Polym. Sci. 79 (2001) 1685–1692.

[29] R.Y.M. Huang, P. Shao, C.M. Burns, X. Feng, Sulfonation of poly(ether ether ketone) (PEEK): kinetic study and characterization, J. Appl. Polym. Sci. 82 (2001) 2651–2660.

[30] Z. Gaown, Z. Zhentao, Organic/inorganic composite membranes for application in DMFC, J. Membr. Sci. 261 (2005) 107–113.

[31] B.P. Tripathi, M. Kumar, V.K. Shahi, Organic–inorganic hybrid alkaline membranes by epoxide ring opening for direct methanol fuel cell applications, J. Membr. Sci. 360 (2010) 90–101.

[32] L. Gubler, S.M. Dockheer, W.H. Koppenol, Radical ($^{\bullet}$OH, $^{\bullet}$H and $^{\bullet}$OOH) formation and ionomer degradation in polymer electrolyte fuel cells, J. Electrochem. Soc. 158 (2011) B755–B769.

[33] B.P. Tripathi, V.K. Shahi, 3-(3-(triethoxysilyl)propylamino)propane-1-sulfonic acid-poly(vinyl alcohol) cross-linked zwitterionic polymer electrolyte membranes for direct methanol fuel cell applications, ACS Appl. Mater. Interf. 1 (2009) 1002–1012.

[34] H. Cerfontain, Mechanical aspect in aromatic sulfonation desulfonation, Wiley-Interscience, New York, 1968.

[35] R.W. Kopitzke, C.A. Linkous, G.L. Nelson, Thermal stability of high temperature polymers and their sulfonated derivatives under inert and saturated vapor conditions, Polym. Degrad. Stab. 67 (2000) 335–344.
[36] A. Carbone, R. Pedicini, G. Portale, A. Longoc, L. DIlario, E. Passalacqua, Sulphonated poly(ether ether ketone) membranes for fuel cell application: thermal and structural characterisation, J. Power Sources 163 (2006) 18–26.
[37] M. Han, G. Zhang, K. Shao, H. Li, Y. Zhang, M. Li, S. Wang, H. Na, Carboxyl-terminated benzimidazole-assisted cross-linked sulfonated poly(ether ether ketone)s for highly conductive PEM with low water uptake and methanol permeability, J. Mater. Chem. 20 (2010) 3246–3252.
[38] R.T.S.M. Lakshmi, V. Choudhary, I.K. Varma, Sulphonated poly(ether ether ketone): synthesis and characterisation, J. Mater. Sci. 40 (2005) 629–636.
[39] C. Zhao, H. Lin, K. Shao, X. Li, H. Ni, Z. Wang, H. Na, Block sulfonated poly(ether ether ketone)s (SPEEK) ionomers with high ion-exchange capacities for proton exchange membranes, J. Power Sources 162 (2006) 1003–1009.
[40] J. Fang, P.K. Shen, Quaternized poly(phthalazinon ether sulfone ketone) membrane for anion exchange membrane fuel cells, J. Membr.Sci. 285 (2006) 317–322.
[41] G. Socrates, Infrared Characteristic Group Frequencies, Wiley, New York, 1980.
[42] J. Pan, S. Lu, Y. Li, A. Huang, L. Zhuang, J. Lu, High-performance alkaline polymer electrolyte for fuel cell applications, Adv. Funct. Mater. 20 (2010) 312–319.
[43] N. Lakshminarayaniah, Transport Phenomenon in Membrane, Academic Press, New York, London, 1969 226–227.
[44] Q.H. Zeng, Q.L. Liu, I. Broadwell, A.M. Zhu, Y. Xiong, X.P. Tu, Anion exchange membranes based on quaternized polystyrene-block-poly(ethylene-ran-butylene)-block-polystyrene for direct methanol alkaline fuel cells, J. Membr. Sci. 349 (2010) 237–243.
[45] Y. Xiong, Q.L. Liu, Q.H. Zeng, Quaternized cardo polyetherketone anion exchange membrane for direct methanol alkaline fuel cells, J. Power Sources 193 (2009) 541–546.
[46] Y. Luo, J. Guo, C. Wang, D. Chu, Quaternized poly(methyl methacrylate-*co*-butyl acrylate-*co*-vinylbenzyl chloride) membrane for alkaline fuel cells, J. Power Sources 195 (2010) 3765–3771.
[47] E.D. Wang, T.S. Zhao, W.W. Yang, Poly (vinyl alcohol)/3-(trimethylammonium) propyl-functionalized silica hybrid membranes for alkaline direct ethanol fuel cells, Int, J. Hydrogen Energy 35 (2010) 2183–2189.
[48] Y. Xiong, J. Fang, Q.H. Zeng, Q.L. Liu, Preparation and characterization of cross-linked quaternized poly(vinyl alcohol) membranes for anion exchange membrane fuel cells, J. Membr.Sci. 311 (2008) 319–325.
[49] N.P. Gnusin, V.I. Zabolotsky, V.V. Nikonenko, M.R. Urtenov, Convection-diffusion model of electrodialysis desalination process, Limiting Current and Diffusion Layer, Elektrokhimiya 22 (1986) 298–302.
[50] V.I. Zabolotsky, V.V. Nikonenko, Effect of structural membrane in homogeneity on transport properties, J. Membr.Sci. 79 (1993) 181–198.
[51] L. Chaabane, L. Dammak, V.V. Nikonenko, G. Bulvetre, B.J. Auclair, The influence of absorbed methanol on the conductivity and on the microstructure of ion-exchange membranes, J. Membr. Sci. 298 (2007) 126–135.
[52] J.H. Choi, S.H. Kim, S.H. Moon, Heterogeneity of ion-exchange membranes: the effects of membrane heterogeneity on transport properties, J. Colloid Interface Sci. 241 (2001) 120–126.
[53] N.P. Gnusin, N.P. Berezina, N.A. Kononenko, O.A Dyomina, Transport structural parameters to characterize ion exchange membranes, J. Membr. Sci. 243 (2004) 301–310.
[54] X.T. Le, P. Viel, D.P. Tran, F. Grisotto, S. Palacin, Surface homogeneity of anion exchange membranes: a chronopotentiometric study in the overlimiting current range, J. Phys. Chem. B 113 (2009) 5829–5836.
[55] N. Pismenskaia, P. Sistat, P. Huguet, V. Nikonenko, G. Pourcelly, Chronopotentiometry applied to the study of ion transfer through anion exchange membranes, J. Membr. Sci. 228 (2004) 65–76.
[56] E. Volodina, N. Pismenskaya, V. Nikonenko, C. Larchet, G. Poucelly, Ion transfer across ion-exchange membranes with homogeneous and heterogeneous surfaces, J. Colloid. Interface Sci. 285 (2005) 247–258.
[57] L.X. Tuan, M. Verbanck, C.B. Herman, H.D. Hurwitz, Properties of CMV cation exchange membranes in sulfuric acid media, J. Membr. Sci. 284 (2006) 67–78.
[58] E.I. Belova, G.Y. Lopatkova, N.D. Pismenskaia, V.V. Nikonenko, C. Larchet, G. Pourcelly, Effect of anion-exchange membrane surface properties on mechanisms of overlimiting mass transfer, J. Phys. Chem. B 110 (2006) 13458–13469.
[59] A.J. Bard, L.R. Faulkner, Electrochemical methods, fundamentals applications, 2nd ed., John Wiley & Sons, Inc., New York, 2001.
[60] F. Helfferich, Ion Exchange, McGraw-Hill Book Co., New York, 1962.
[61] T. Sata, Studies on anion exchange membranes having permselectivity for specific anions in electrodialysis-effect of hydrophilicity of anion exchange membranes on permselectivity of anions, J. Membr. Sci. 167 (2000) 1–31.
[62] V.M.M. Lobo, J.L. Quaresma, Hand Book of Electrolyte Solutions, Elsevier, New York, 1989.